

# On the origin of complexity in PKP travel time data.

B. Romanowicz<sup>1</sup>, H. Tkalčić<sup>2</sup>, L. Bréger<sup>3</sup>

## Abstract.

In order to investigate the origin of short spatial scale features in PKP travel time data and to determine whether a complex inner core anisotropy model is required, we have assembled a new global dataset of handpicked absolute PKP(DF) travel times, and completed existing datasets of handpicked relative PKP(AB-DF) and PKP(BC-DF) travel times. We discuss in detail the trends of relative and absolute PKP travel time residuals at the global scale, as well as for a well sampled set of paths between the south Atlantic and Alaska.

We discuss the relative merits of several types of models: a) a model of hemispherical anisotropy in the inner core previously proposed to explain PKP(BC-DF) travel time residuals on the global scale; b) a model combining weak constant anisotropy in the inner core with strong heterogeneity in the deep mantle; c) a model involving structure in the outer core associated with the tangent cylinder to the inner core, with axis parallel to the rotation axis, a feature described in magnetohydrodynamical models of the outer core.

Because absolute PKP(DF) travel time residuals exhibit the same hemispherical pattern as relative PKP(BC-DF) and PKP(AB-DF) data, when plotted at the location of the bottoming point of DF in the inner core, we infer that the causative structure must at least partly originate in the core. However, the transition between anomalous and normal structure is quite abrupt, and hemispherical inner core anisotropy models fail to reproduce the characteristic "L shape" of PKP(BC-DF) travel time residuals, when plotted as a function of the angle of the ray in the inner core with the rotation axis ( $\xi$ ). Models involving mantle heterogeneity compatible with other mantle sensitive data can explain PKP(AB-DF) travel times, but fail to explain 3 sec of average PKP(BC-DF) anomaly observed for paths bottoming in the western hemisphere, for  $\xi \sim 20 - 30^\circ$ , even when a model of constant anisotropy in the inner core, compatible with mode splitting data, is also included. On the other hand, models with  $\sim 1\%$  faster velocity inside an outer core region roughly delimited by the inner core tangent cylinder allow for rapid transitions, are compatible with trends in absolute PKP(DF) and PKP(BC) times observed in Alaska, and can reproduce the L-shaped feature of the PKP(BC-DF) travel time data. Sustained heterogeneity in the outer core could arise within polar vortices in and around the tangent cylinder, as suggest by recent dynamical and magnetic investigations. Such models are also compatible with most normal mode splitting data and present less departure from axial symmetry than the hemispherical inner core anisotropy models. When trying to physically explain them, both types of models present challenges, and should be pursued further.

## 1. Introduction

The first observation that PKP(DF) waves travel faster through the earth's inner core along polar paths (paths quasi-parallel to the earth's rotation axis) than on equatorial paths, was made almost 20 years ago (Poupinet et al., 1983). Subsequently, it was proposed that this could be due to inner core anisotropy, which would explain the

PKP observations (Morelli et al., 1986) as well as observations of anomalous splitting of core sensitive free oscillations (Masters and Gilbert, 1981; Woodhouse et al., 1986). These observations were later confirmed in many studies, both for PKP travel times (e.g. Shearer et al., 1988; Shearer, 1991; Creager, 1992; Vinnik et al., 1994; Su and Dziewonski, 1995; Song, 1996) and for core modes (Ritzwoller et al., 1988; Li et al., 1991).

The early inner core anisotropy models were cast in terms of constant transverse isotropy with fast axis parallel to the earth's axis of rotation, as would be expected if the anisotropy were due to the alignment of hcp-iron crystals with the axis of rotation (e.g. Stixrude and Cohen, 1995). Proposed physical mechanisms for anisotropy have involved convection in the inner core (Jeanloz and Wenk, 1988), magnetic effects (Karato, 1995, 1999), gravitational interaction with the mantle (e.g. Buffett and Creager, 1999) or texturing of iron during inner core solidification (Bergman,

<sup>1</sup>Seismological Laboratory, University of California, Berkeley.

<sup>2</sup>Now at: IGPP, University of California, San Diego

<sup>3</sup>Now at: BARRA, Berkeley, CA

1997). Most of these mechanisms, except perhaps gravitational interaction in the mantle, imply axisymmetry of the anisotropic structure.

As data have accumulated and revealed more details, inner core anisotropy models have become more complex. Depth dependence of the strength of anisotropy was proposed (Su and Dziewonski, 1995; Tromp, 1993) and helped explain a long standing discrepancy between the travel time and mode observations (Tromp, 1995), even better so when departures from a simple radial model are also considered (Romanowicz et al., 1996). To explain strong anomalies for polar paths in northeastern Eurasia and Alaska, it was proposed that the axis of symmetry of the anisotropy could be tilted with respect to the earth's axis of rotation (Su and Dziewonski, 1995; McSweeney et al., 1997), but Souriau et al. (1997) demonstrated that this result was not statistically robust, due to the uneven sampling of the globe by the PKP data. The most intriguing observation to date, in our opinion, was made by Tanaka and Hamaguchi (1997), who observed that only one hemisphere, extending roughly from longitude  $177^\circ W$  to  $43^\circ E$  ("Quasi-western" hemisphere) was anisotropic, a fact later confirmed by Creager (1999), who noted that the strength of anisotropy was different in the two hemispheres, but both supported the same Voigt average velocity. On the other hand, Song and Helmberger (1998) proposed that the top of the inner core is isotropic and separated from the central anisotropic part by a discontinuity of varying depth. However, the isotropic part cannot be, on average, thicker than 100-200 km, to account for constraints from anomalous splitting of core sensitive modes (Durek and Romanowicz, 1999). In order to account for the difference in the two hemispheres, as well as the existence of an isotropic region at the top of the inner core, Creager (2000) and Garcia and Souriau (2000) recently proposed very similar models which comprise a discontinuity within the inner core, separating an isotropic outer core from an anisotropic inner core. The ellipsoidal shape of this discontinuity is shifted with respect to the center of the inner core, so that the isotropic part is thicker in the eastern (400km) than in the western ( $< 100km$ ) quasi-hemisphere.

Other complexities in the PKP(BC-DF) and PKP(AB-DF) travel time data have recently been documented by Bréger et al. (1999, 2000a,b), who pointed out how important it is to account accurately for the influence of strong heterogeneity at the base of the mantle, before making inferences on inner core anisotropy from the observation of core sensitive phases. It is difficult to find physical mechanisms to explain the increasingly complex structure of the inner core anisotropy required by recently accumulated high quality broadband data, and in particular, the hemispherical differences, given that the inner core is thought to be close to the melting point of its constituents. In view of the mounting evidence for strong heterogeneity in the deep mantle (e.g. Garnero and Helmberger, 1996; Bréger and Romanowicz, 1998; Ritsema et al., 1998) and the uneven distribution of PKP observations on polar paths around the globe (Bréger et al., 2000a), it is important to consider whether the complexity originates in the inner core or elsewhere, and whether it might all be accounted for by mantle structure.

In what follows, we discuss possible origins of the most significant, first order features of PKP travel time data, measured on the rapidly growing collection of short period and broadband records, at the global scale, and also, more specifically, for a set of intriguing paths between the south-Atlantic and Alaska.

## 2. Description of the datasets and some specific trends

We have assembled a comprehensive dataset comprising PKP(AB-DF), PKP(BC-DF) differential travel times, and PKP(DF) absolute travel times, which we measured on vertical component records from broadband and short period stations worldwide for the time period 1990-1998 (Tkalčić et al., 2002), and complemented by datasets collected by sev-

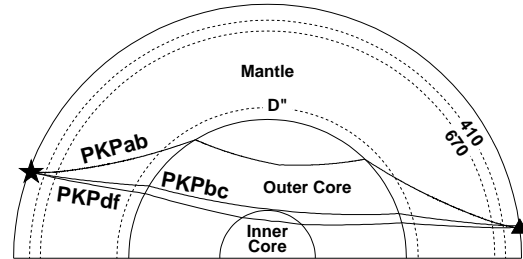


**Figure 1.** Vertical cross-section through the earth showing the paths of the three PKP phases

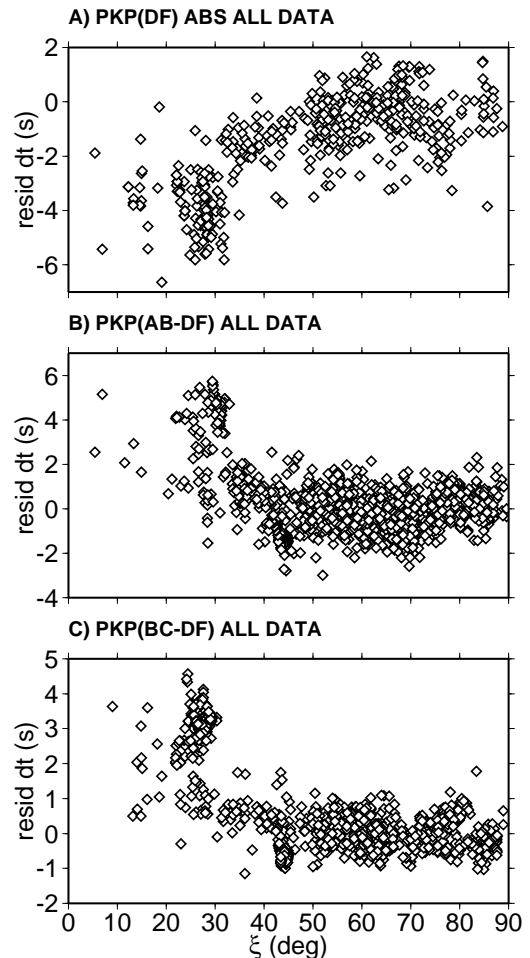


**Figure 2.** Variations of travel time residuals for PKP (DF) (absolute measurements, top), PKP(BC-DF) (middle) and PKP(AB-DF) (bottom) as a function of the angle  $\xi$  made by the inner core leg of the path with the earth's rotation axis. Residuals are referred to model AK135 and have been corrected for ellipticity.

eral other authors. The geometry of the various PKP phases is shown in Figure 1.

We measured differential travel times by cross-correlation of the two phases involved. The details of the measurement technique are given in Tkalčić et al. (2002). The complete dataset combines our data with those of McSweeney et al. (1997), Creager (1999), Tanaka and Hamaguchi (1997), Souriau (personal communication) and Wyession (personal communication). These data have been carefully inspected for inconsistencies between authors, duplications, and errors. In particular, we made systematic plots of variations as a function of back-azimuth for groups of neighboring stations, as well as variations as a function of azimuth for groups of neighboring events. This allowed us to eliminate clear outliers, but it was possible only for equatorial and quasi-equatorial paths ( $\xi > 35^\circ$ ), for which data are numerous. The corresponding differential travel times consistently show variations around the mean not exceeding  $\pm 2.5 \text{ sec}$  for PKP(AB-DF), and  $\pm 1.5 \text{ sec}$  for PKP(BC-DF). The error in measurement for these equatorial paths is estimated to be  $\leq 0.5 \text{ sec}$  and we were able to eliminate practically all residuals exceeding respectively  $\pm 2.5 \text{ sec}$  (AB-DF) and  $\pm 1.0 \text{ sec}$

(BC-DF) as outliers. For polar paths, data are fewer, so that this type of verification is not possible. We note however that, for quasi-polar paths ( $\xi < 35^\circ$ ) for which numerous measurements are available, such as at stations of the dense Alaska network, there are indications of consistent variations over short distances, as we will discuss further below.

We also measured absolute PKP(DF) travel times, whenever possible, and present this new dataset here for the first time. The distance range spanned by the data is  $145^\circ$  to  $175^\circ$ . For these measurements, we cannot take advantage of the accuracy of waveform comparison, and we must rely on direct picks of the onset of the DF phase, which is often emergent, especially for polar paths. Therefore, the measurement error is larger in general, on the order of  $1 \text{ sec}$  for equatorial paths, and up to  $2 \text{ sec}$  in some cases, for polar paths. We thus expect a larger scatter in the data. However, absolute measurements are of great interest for the study of inner core anisotropy, and are the basis of most inferences made using data collected from ISC bulletins (e.g. Poupinet et al., 1983; Morelli et al., 1986; Shearer, 1988; Su and Dziewonski, 1995). Moreover, global variations in absolute DF (in particular differences between polar and equatorial paths) are largely in excess of the measurement error.

Figure 2 shows the variations, as a function of angle  $\xi$ , of PKP(BC-DF), PKP(AB-DF) and PKP(DF) travel time

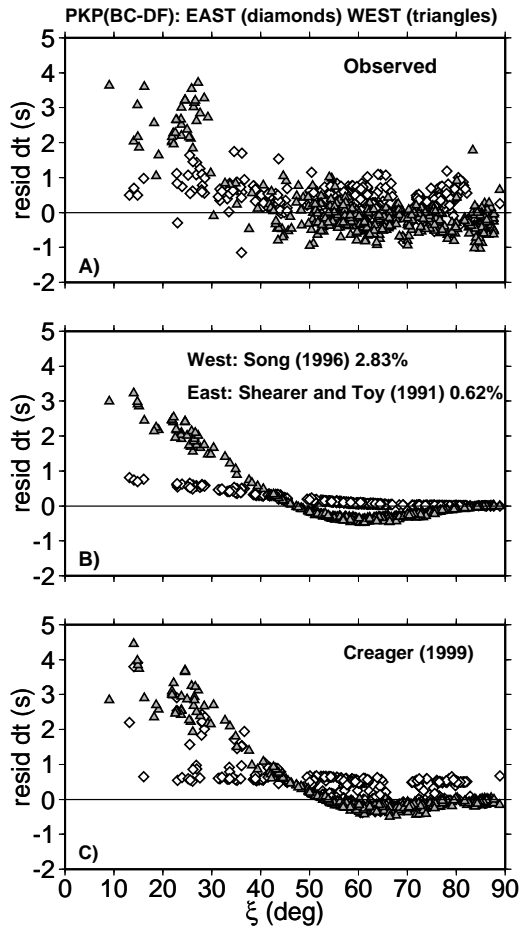


**Figure 3.** PKP(BC-DF) travel time residuals as a function of  $\xi$ , distinguishing quasi-eastern (diamonds) and quasi-western (triangles) hemispheres. A) Observed; B) predictions of two different models of constant transverse isotropy in the inner core (strength indicated); C) Predictions of Creager's (2000) off-centered hemispherical inner core anisotropy model. In this plot, Alaska network data have been replaced by summary rays.

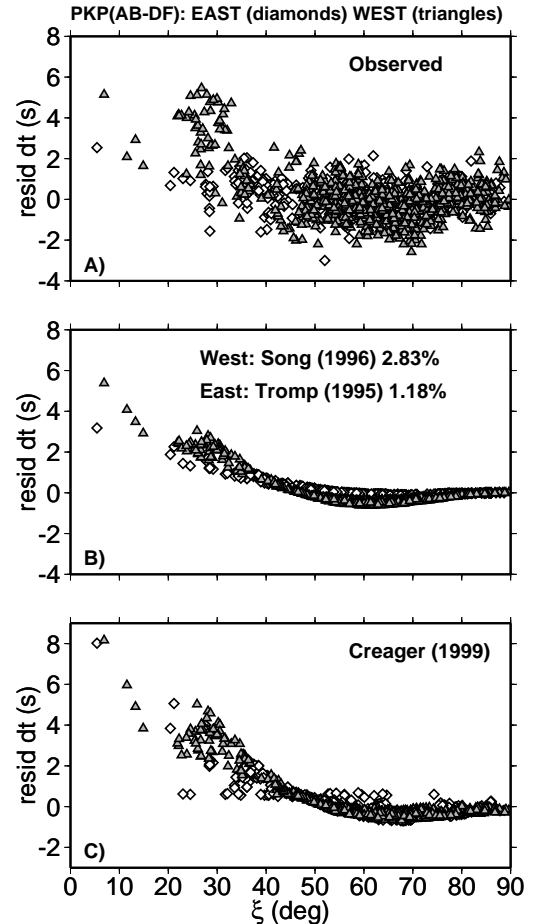


**Figure 4.** Same as Figure 3 for the PKP(AB-DF) dataset. Note that a slightly stronger anisotropy model is plotted in B) for the eastern hemisphere.

residuals, referenced to model AK135 (Kennett and Engdahl, 1991), and corrected for ellipticity. The epicentral data used in the computation of residuals are those from the EHB catalog (Engdahl et al., 1998). We note the larger scatter of the DF data, as expected, and the large spread of values for  $\xi \leq 35^\circ$ . On average, residuals are several seconds larger for polar paths than for equatorial paths, consistent with all previous studies. The raw datasets, however, do not exhibit a smooth variation with  $\xi$  as would be expected for simple models of inner core anisotropy. Rather, the curves are L-shaped and there is a sharp break around  $\xi = 30^\circ$ , with many residuals larger by 2-4 sec for the more polar paths. Several events in the south Atlantic (south Sandwich Islands in the BC-DF distance range and Bouvet Islands in the AB-DF distance range) observed at stations of the Alaska network contribute to the large concentration of data points for  $20^\circ \leq \xi \leq 30^\circ$  and exhibit a large scatter, which has been attributed to heterogeneity in the inner core (e.g. Creager, 1997; Song, 2000). We will discuss these data in detail. The distinct "line" of negative anomalies between 0 and -1 sec, around  $\xi = 43^\circ$ , in the BC-DF dataset, (also present in the AB-DF dataset) corresponds to the 03/29/1993 South Atlantic earthquake observed on the dense California short period networks.

In Figure (3a), we show the variations with  $\xi$  of the PKP(BC-DF) travel time residuals, after replacing the two clusters mentioned above by summary rays, and distinguishing the quasi-eastern and quasi-western hemispheres, according to the definition of Tanaka and Hamaguchi (1997). Indeed, we confirm the differences in trends for both hemispheres, with practically no dependence with  $\xi$  in the quasi-eastern hemisphere. As noted previously (Tanaka and Hamaguchi, 1997; Creager, 1999), there is also a difference of 1 sec on average, for non polar angles  $\xi$ , between BC-DF residuals in the quasi-eastern and quasi-western hemispheres,

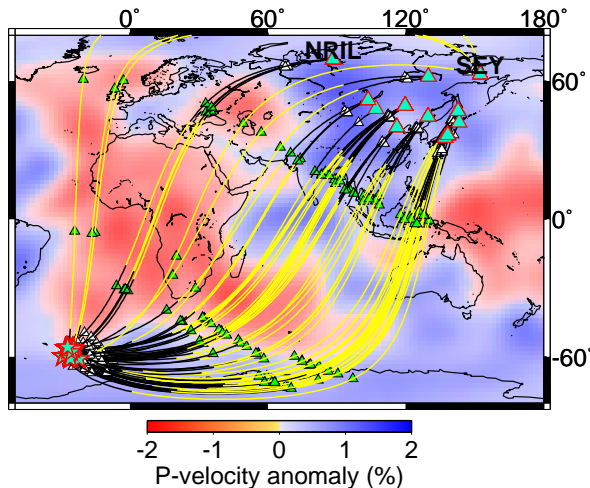


**Figure 5.** Surface projections of PKP wavepaths from sources in south Sandwich Islands to stations in Eurasia. Yellow thick lines correspond to the inner core legs of PKP. We also plotted the points where PKP enter and exit the outer core (white and green triangles). Model PAW24B16, obtained by converting S-velocity model SAW24B16 [Mégnin and Romanowicz, 2000] into a P-velocity model using the scaling relation  $d \ln V_s / d \ln V_p = 2$ , is used as background.

with the former being faster. For comparison, we plot, in Figure (3bc), the predictions of two inner core anisotropy models that provide good fits to the average observed trends. In Figure 3b, the predictions for each hemisphere are calculated separately for two constant anisotropy models proposed in the literature. The quasi-eastern hemisphere could support anisotropy in the inner core of strength less than 1%, whereas the anisotropy required to explain data in the quasi-western hemisphere is close to 3%. In Figure 3c, we show the predictions of Creager's (2000) 2-layer model of the inner core. Some slight discrepancies in the location of the boundary between the eastern and western parts of the model are apparent, but on average this model fits the trends in the data well to first order. However, in the western hemisphere, both models (3b, 3c) overestimate the residuals observed in the range  $\xi = 30 - 35^\circ$ , and underestimate them in the range  $\xi = 20 - 30^\circ$ , indicating that significant features in the data, namely the L shape rather than smooth increase of residuals as a function of  $\xi$ , are not explained by hemispherical anisotropy.

In Figure 4, we present the results of the same analysis for the PKP(AB-DF) dataset. In this case, the constant anisotropy required in the quasi-eastern hemisphere (Figure 4b) is stronger than for PKP(BC-DF). On the other hand, the western hemisphere model with 2.83% anisotropy underestimates the dispersion of the residuals in the  $\xi = 20 - 30^\circ$  range by a factor of two. A model with 3.5% anisotropy would fit the data in this range better, but would overestimate the residuals at smaller angles. Creager's hemispherical model (Figure 4c) underestimates residuals in the range  $\xi = 20 - 30^\circ$  by 1-2 sec and overestimates the residuals at  $\xi < 20^\circ$  by up to 2.5 sec. Inspection of the data shows that, unlike for BC-DF, there is no clear distinction in the data between eastern and western hemispheres at  $\xi > 35^\circ$  (non polar paths).

### 3. Complex inner core anisotropy or strong heterogeneity at the base of the mantle?

In the previous section, we discussed how hemispherical models of inner core anisotropy can reproduce some of the trends in the PKP travel time data, but fail to reproduce the characteristic "L-shape" of the variations of residuals with angle  $\xi$ . Here we consider the possible contribution of heterogeneity at the base of the mantle. As is now well established, lateral heterogeneity increases and changes style in the last few hundred kilometers above the core mantle boundary (CMB), reaching rms variations in S velocity in excess of 2% in  $D''$ . Although recent S tomographic models differ from each other in their details, they all agree that the spectrum of heterogeneity changes from white to red at the bottom of the mantle, where degree 2 predominates (e.g. Masters et al., 1996; Grand, 1997; Liu et al., 1998; Mégnin and Romanowicz, 2000; Ritsema et al., 2000), with a distinctive spatial pattern showing two large low velocity regions under Africa and in the central Pacific, surrounded by a "ring" of fast velocities, as first shown in Dziewonski et al. (1977). While S tomographic models successfully retrieve the large scale patterns of heterogeneity, they underestimate the strength of lateral variations, at least in some regions, by a factor of 2 or 3, as has been shown by comparison of observed and predicted differential travel time anomalies of S-SKS and Sdiff-SKS waves, in the well sampled "corridor" across the Pacific Ocean (Bréger et al., 1998), as well

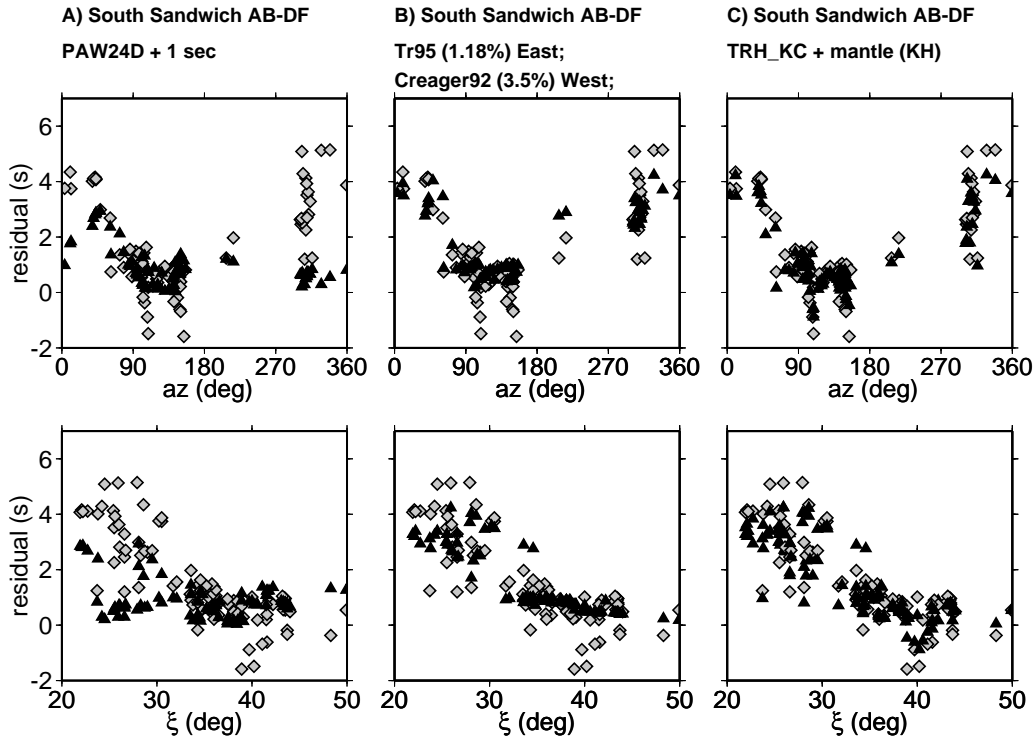


**Figure 6.** Variations as a function of  $\xi$  (bottom) and Azimuth (top) of observed PKP(AB-DF) travel time residuals for south Sandwich Island events. Comparisons with predictions are shown for A) mantle model PAW12B16 shifted upward by 1sec; B) hemispherical inner core anisotropy model: Tromp (1995) in the quasi eastern hemisphere and Creager (1992) in the quasi-western hemisphere; C) mantle model combining a tomographic model (Karason and van der Hilst, 2001) down to 300km above the CMB and the D” model *TRH\_KC* of Tkalčić et al. (2002).

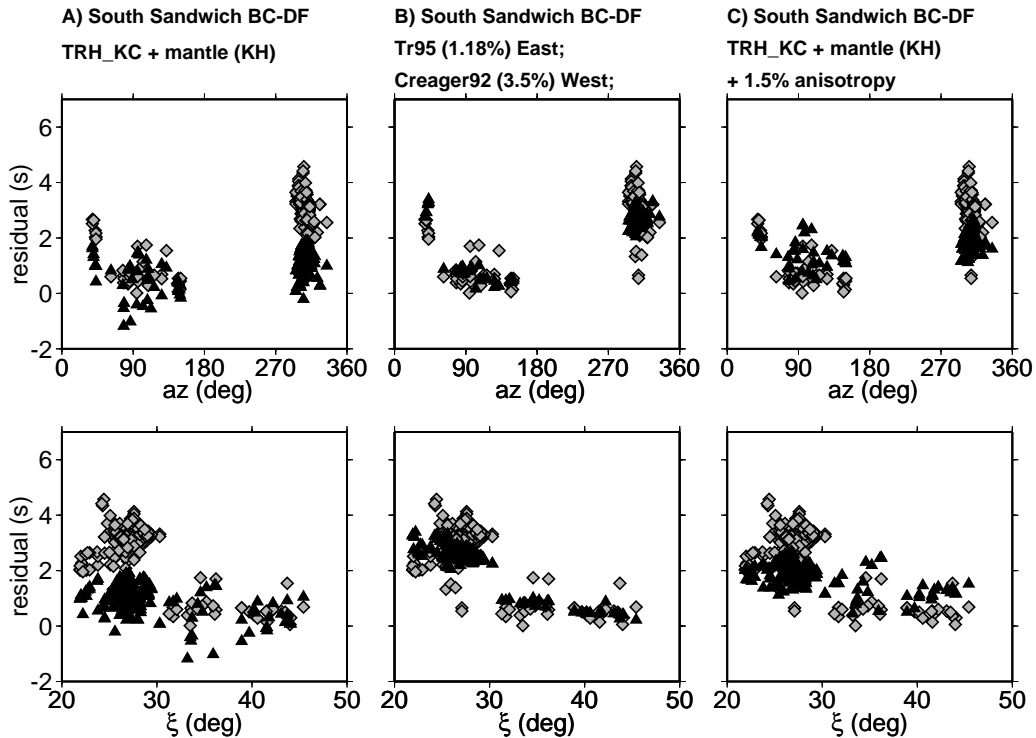


**Figure 7.** Same as Figure 6 for PKP(BC-DF) observations and predictions: A) *TRH\_KC* model (Tkalčić et al., 2002); B) Hemispherical inner core anisotropy model; C) *TRH\_KC* plus constant inner core anisotropy model of strength 1.5% (Romanowicz and Bréger, 2000).

al., 1998; Ni and Helmberger, 1999) have documented strong gradients in the regions bordering these plumes in D", with lateral variations in excess of  $\pm 5\%$  over distances of 200-400km. While not necessarily completely correlated, similar characteristics are expected in the P velocity distribution at the base of the mantle. Indeed, PcP-P data at large distances confirm the presence of short wavelength variations of at least  $\pm 2\%$  in some well sampled regions (Tkalčić et al., 2002). In addition, there is evidence for regions of localized ultra low velocities (ulvz's), with P velocity anomalies in excess of 10% (e.g. Garnero and Helmberger, 1996). Recently, Bréger et al. (2001) showed that, by considering an existing tomographic model of the mantle (Grand, 1997) increasing the amplitude of lateral variations in D" and including ulvz's, a significant portion of the trend with  $\xi$  of PKP(AB-DF) travel time residuals could be explained without even accounting for anisotropy. Indeed, as shown in Figure 1, the PKP(AB) wavepath grazes the core-mantle boundary and thus interacts with structure in D" much more than the corresponding PKP(DF) path. We thus expect, as first pointed out by Sacks et al. (1979) and further considered by Sylvander and Souriau(1996), that PKP(AB-DF) differential travel times may be strongly affected by heterogeneity in D". A major concern is that the distribution of PKP paths in the distance range appropriate for PKP(AB) observations and for angles  $\xi$  smaller than  $40^\circ$  is very non-uniform, with a majority of paths originating in the south Atlantic, specifically in the seismically active region of the south Sandwich Islands (e.g. Bréger et al., 2000a), located near the border of the African superplume.

Figure 5 shows the geometry of paths from south Sandwich Islands to stations in Eurasia. Plotted in the background is a P velocity model (PAW24D) obtained by scaling the tomographic S velocity model SAW24B16 (Mégnin and Romanowicz, 2000) using a ratio  $dl_n V_s / dl_n V_p = 2$ . Indicated are entry points of DF and AB into the core. We note that for north to north-east trending paths, the AB phase interacts with the low velocity "African superplume" structure, whereas the DF phase stays largely outside of it. In Figure 6, we present various attempts at modeling trends in the PKP(AB-DF) travel time residuals, as a function of azimuth or  $\xi$ , for events originating in the south-Sandwich Island region, to stations in Eurasia and Alaska. In Figure 6ab, we compare the PKP(AB-DF) observations with the predictions of tomographic model PAW24D, shifted upward by 1sec (to account for an obvious baseline shift on these paths) and of the hemispherical model of inner core anisotropy, presented in Figure 4. The tomographic model fails to predict the large spread of residuals at azimuths greater than  $270^\circ$ , which correspond to South-Sandwich to Alaska paths. The hemispherical anisotropy model improves the average fit in these azimuths (as well as in the azimuth range  $0 - 40^\circ$ ), but still fails to explain the large scatter in the Alaska data. Finally, in Figure 6c, we show the predictions of a D" model ( $TRH_{KC}$ ) constructed by Tkalčić et al. (2002) using a combination of globally distributed PKP(AB-DF) and PcP-P data, corrected for mantle structure using the Karason and vanderHilst (2000) mantle P model to a depth of 300 km above the CMB. Model  $TRH_{KC}$  predicts the scatter in the Alaska data better, as well as the longer wavelength trends with azimuth. In fact, Tkalčić et al. (2002) have shown that over 80% of the variance in the PKP(AB-DF) data can be explained by such a model, without requiring hemispherical anisotropy in the inner core.

While it is not too surprising that PKP(AB-DF) travel time residuals can be explained largely by mantle heterogeneity, especially since model  $TRH_{KC}$  was constructed to

fit such data, additional insight can be gained from the analysis of PKP(BC-DF) data, noting that PKP(BC) and PKP(DF) travel on very close paths throughout the mantle. Figure 7 shows the comparison of observed and predicted PKP(BC-DF) travel time residuals for paths originating in the south-Sandwich Islands, for model  $TRH_{KC}$  (Figure 7a) and the hemispherical inner core model (Figure 7b). We note that the mantle model reproduces a large fraction of the local scatter in the data, but fails to predict the 3 sec average BC-DF travel time anomaly for Alaska paths. On the other hand, the hemispherical inner core anisotropy model does predict 3 sec of BC-DF anomaly in Alaska, but fails to produce the full observed scatter in these data. In Figure 7c, we show the predictions of a model which combines the D" model of Tkalčić et al. (2002) with a constant inner core anisotropy model of about 1.5%. The maximum strength of anisotropy is constrained by the necessity to fit small residuals for azimuths between  $70^\circ$  and  $160^\circ$ . On the other hand, the strength of lateral heterogeneity in D" derived in the models of Tkalčić et al. (2002) is also constrained by the scatter observed in PKP(BC-DF) data on non-polar paths. We see that a model such as shown in Figure 7c fails to predict the average 2.5-3 sec of PKP(BC-DF) residuals on paths from south Sandwich Islands to Alaska.

We infer from Figures 6 and 7 that we cannot completely explain both the local scatter and the large scale variations in the south Sandwich events subset of PKP(BC-DF) by a model of heterogeneity in D" combined with a simple model of constant weak anisotropy in the inner core as might be compatible with normal mode splitting data. For this subset of data, it is necessary to combine D" heterogeneity with inner core anisotropy of at least 3.5%.

#### 4. Different global projections of the PKP travel time residuals

In Figure 8abc, we compare the global distribution of PKP(DF), PKP(DF-AB) and PKP(DF-BC) travel time residuals plotted at the location of the bottoming point of DF in the inner core on the one hand, and on the other, at the entry point of DF into the outer core, in the northern hemisphere. When plotted at the DF bottoming point, (only polar paths, for  $\xi < 40^\circ$  are shown for clarity), all three datasets show the same, well documented quasi-hemispherical pattern. It is important to note that the absolute PKP(DF) residuals also show the hemispherical trend, which, on the other hand, is not clearly present in absolute PKP(BC) times, implying that it likely originates at least partly in the core. There are however notable outliers, in particular for paths to stations in Europe, bottoming at longitudes near  $310^\circ E$  (both in PKP(DF) and PKP(DF-AB)). Also, the cluster of well sampled paths from the south Atlantic to Alaska "hides" many points with small residuals in the western hemisphere (those that account for the spread in residuals for  $20^\circ < \xi < 30^\circ$  in figure 1). The transition from fast to slow in the middle of the Pacific occurs very rapidly, although somewhat further east (by over  $40^\circ$  in longitude) in the PKP(DF-AB) dataset than in the absolute PKP(DF) one.

On the other hand, the projections at the DF entry point into the core for these two subsets show a very similar pattern: except for a few isolated outliers, all the very anomalously fast paths concentrate in the polar region, which is

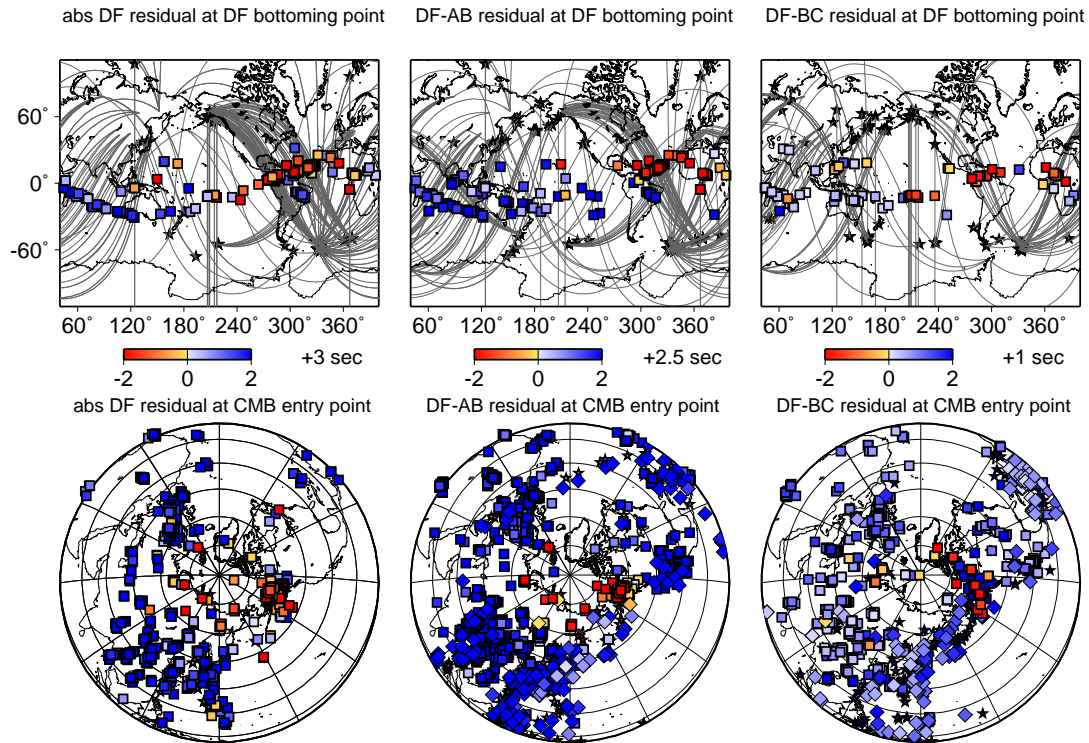


**Figure 8.** Travel time residuals for quasi-polar paths ( $\xi < 40^\circ$ ) plotted at the position of the bottoming point of the path in the inner core (top) and at the entry point into the core in the northern hemisphere (bottom). Left: absolute PKP(DF) residuals; The color code is centered at  $\delta t = -3.0\text{sec}$ ; Middle: PKP(DF-AB) residuals. The color code is centered at  $\delta t = -2.5\text{sec}$ ; Right: PKP(DF-BC) residuals. The color code is centered at  $\delta t = -1.0\text{sec}$ .

unfortunately not well sampled in its center. In particular, in this projection, the cluster of mild residuals (blue) from an event in the central Pacific to stations in Europe is now compatible with other less polar and not anomalous paths to stations in Europe. Not visible at this scale, the cluster of points from south Atlantic to Alaska indicates that the more anomalous paths are on the north pole side, delineating a transition from "normal" to anomalous structure. We will return to this in more detail in Figure 9. The PKP(DF-BC) polar plot (Figure 8c) is compatible with the two previous ones: if heterogeneity located in a polar region is responsible for the observed patterns, one would expect to observe anomalous PKP(DF-BC) only at the border of this region: in its center, both PKP(DF) and PKP(BC) would sense the anomaly, resulting in a small differential residual. Unfortunately, the current sampling of the polar regions is insufficient, due in particular to very noisy data combined with highly attenuated PKP(DF) on polar paths (e.g. Souriau and Romanowicz, 1996). Whether or not the anomalous structure involves the entire "polar cap" is not clear at this point, but we note that, in any case, it requires much less departure from axial symmetry in the core, than the hemispherical inner core anisotropy model.

In Figure 9, we show in more detail the distribution of absolute DF and absolute BC travel time anomalies, plotted at the entry point of the rays into the core, for 5 south-Sandwich events, and two events located further east in the south Atlantic (90/04/30 Bouvet Island event: latitude =  $-54.34^\circ$ ; longitude =  $1.341^\circ$ , depth = 7.7 km and 96/09/20 event south of Africa: latitude =  $-53.01^\circ$ ; longitude =  $9.855^\circ$ , depth = 6.7 km), recorded on the Alaska network,

from which we were able to obtain waveforms with clear onsets of PKP(DF) and PKP(BC) or PKP(AB) (courtesy of R. Hansen). Figure 9 illustrates the rapid transition from normal to strongly anomalous paths from south-east to north-west under northwestern Canada and Alaska. Except for one point around  $lat = 49^\circ, lon = -143^\circ$  (where the DF measurement is for an Alaska event observed at SPA and the BF measurement for a south Sandwich Island event observed in Alaska), both DF and BC (and AB) absolute times are compatible with a structure trending SW-NE, located near the CMB, with a strong gradient from fast to slow in the NW to SE direction. This structure could be a quasi-vertical "slab" of high velocity in the deep mantle, which would need to be very thin to be as yet undetected by standard mantle tomographic approaches. However, it could also be on the core side, which would in particular make the DF and BC observations even more compatible. Thus, the non-incompatibility of the BC data (crosses) and the DF data (circles) suggests that an origin outside of the inner core, for these anomalies, is not inconceivable, in contrast to inferences made by Creager (1997) and Song (2000) based on the analysis of differential BC-DF and AB-DF travel times from these events.

Figure 10 shows a closer view of the trends of absolute DF (diamonds) and absolute BC (triangles) as a function of  $\xi$ , azimuth and epicentral distance, for the 5 south Sandwich Island events which we measured. The patterns seen in Figure 10 confirm that the BC residuals track the DF residuals, when plotted on the station side, although spatial variations have smaller amplitudes, and the trend is clearest in the plots as a function of epicentral distance. This cannot be explained by structure on the source side, where the

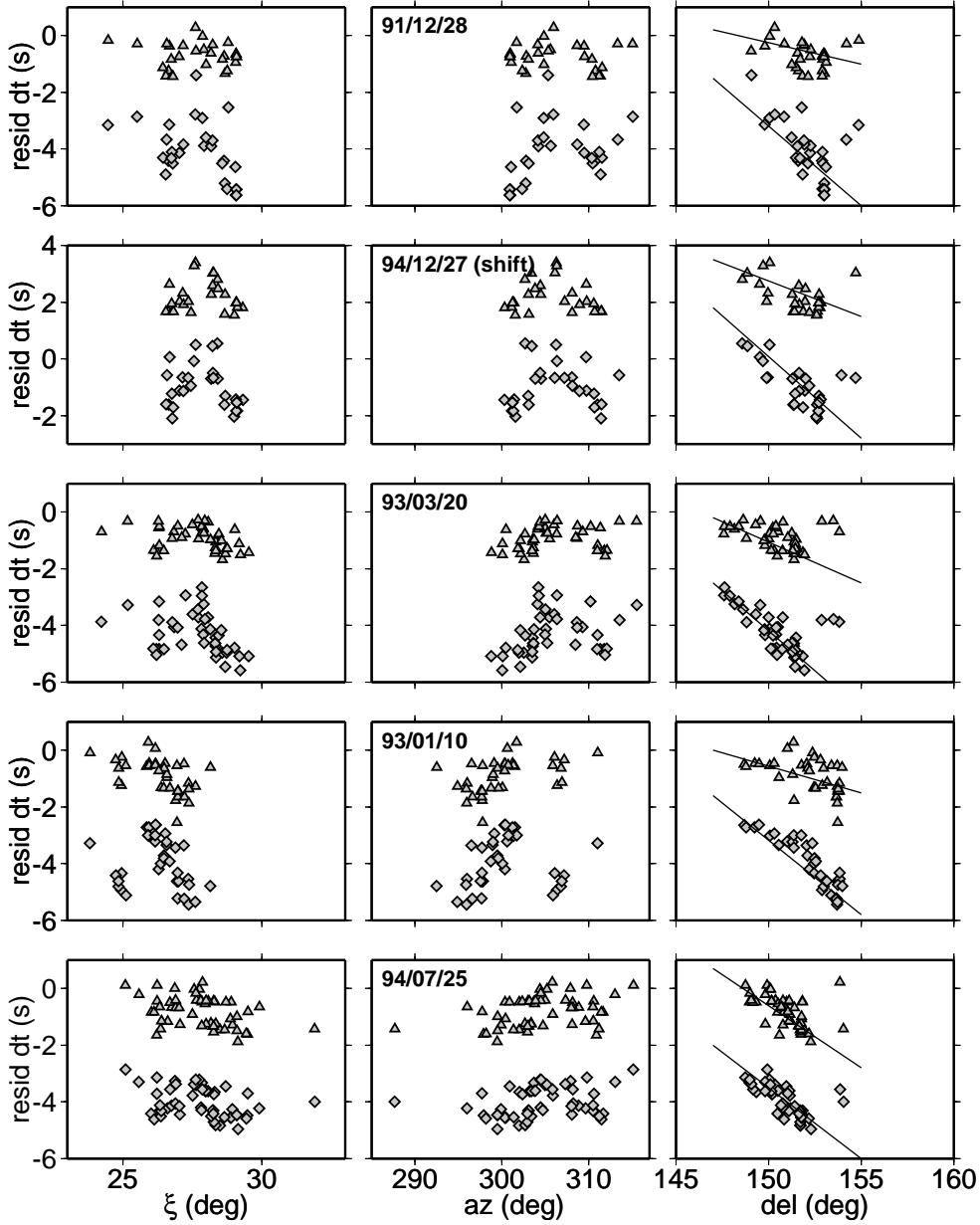


**Figure 9.** Absolute PKP(DF) (diamonds) and absolute PKP(BC) (triangles) travel time residuals measured across the Alaska network for five of the south Sandwich Islands events discussed in the text, plotted as a function of  $\xi$  (left), azimuth (middle) and epicentral distance (right). Note that for the 91/12/27 event, all absolute measurements have to be shifted by +3 sec, probably due to an error in the relocated epicentral parameters.

azimuthal spans of these events partially overlap, as shown in Figure 11. On the other hand, because the variation with epicentral distance is smaller for BC than for DF, a residual trend is observed in the DF-BC data (Figure 12). When considering differential travel times, uncertainties in source location or depth, as well as near source and near station effects are eliminated. Because a similar trend is observed in absolute BC, the structure responsible for the variations with epicentral distance in PKP(DF-BC) should be outside of the inner core.

Figures 8-12 thus indicate that the transition from normal to anomalous paths happens over very short spatial scales. If the anomalous region is in the inner core, then a hemispher-

ical model is necessary, and a physical explanation needs to be found for such an improbable structure. On the other hand, heterogeneity outside of the inner-core remains a possibility. We cannot rule out the possible contribution to observations in Alaska from a thin quasi-vertical slab in the lower mantle.

## 5. Possible alternative models to the hemispherical inner core anisotropy

In previous sections we have seen that it is difficult to explain PKP(BC-DF) travel time residuals with a realistic global mantle model that would not violate constraints from splitting of modes sensitive to mantle structure (e.g. Ro-

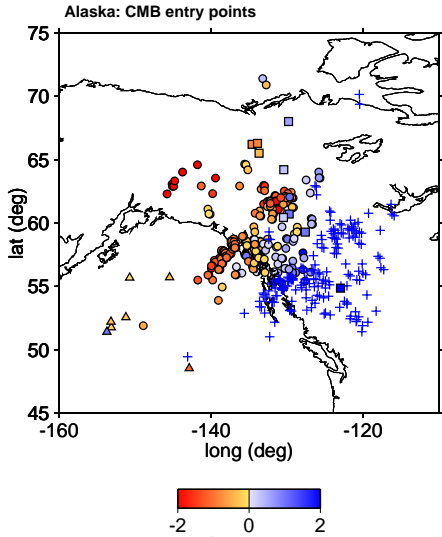
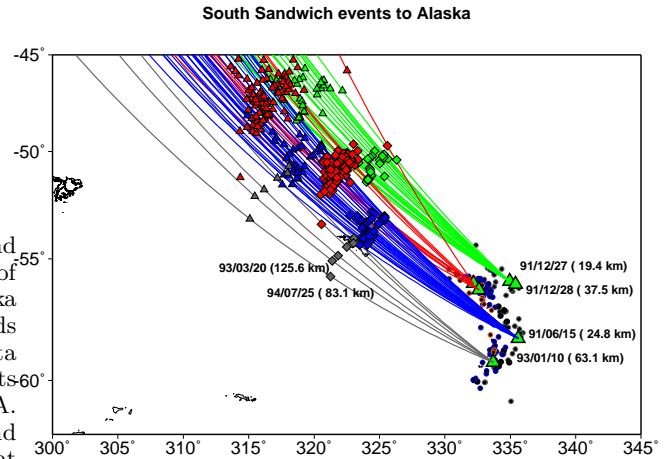


**Figure 10.** Absolute PKP(DF) residuals (full symbols) and PKP(BC) and PKP(AB) residuals (crosses) as a function of position of the DF entry point into the core on the Alaska side, for different events in the south Sandwich Islands and south Atlantic. 90/04/30 Bouvet Island event DF data are indicated by squares. Also shown are DF entry points for events in Alaska observed at south pole station SPA. The colors indicate relative values of the residual around the mean for each event and the color code is centered at  $\delta t = -3.5$  sec.

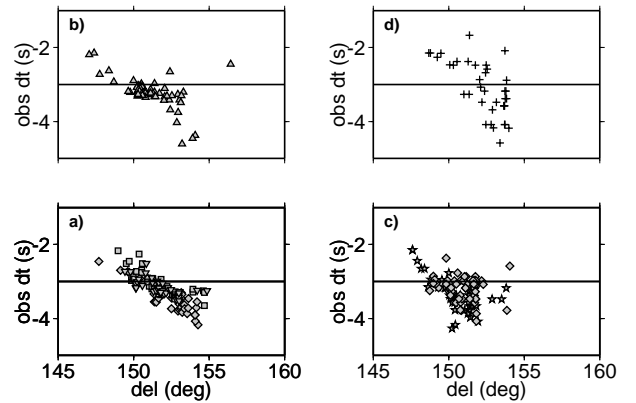
manowicz and Bréger, 2000), that a hemispherical model of inner core anisotropy is the simplest explanation for strongly anomalous PKP data on polar paths, but shows some inconsistencies, and that there are indications from the data, in particular from the dense recordings of south-Atlantic events in Alaska that at least part of the anomaly could originate in the vicinity of the core-mantle boundary. We have previously argued that models that allow outer core heterogeneity, as first proposed by Ritzwoller et al. (1986) and Widmer et al. (1992) could provide an alternative explanation for the strongly anomalous PKP travel time data, as well as splitting data for most normal modes sensitive to core structure. Here we further argue that a hypothetical structure bounded approximately by the cylinder tangent to the inner core, with axis parallel to the earth's rotation axis, a region singled out in models of core dynamics (e.g. Hollerbach and Jones, 1995; Olson et al., 1999) could create the types of trends observed in the data (e.g. Romanowicz and Bréger, 2001). Within the anomalous region, bounded by the tangent cylinder, P velocity would be about 1% faster than outside.

Figure 13 shows a comparison of the global PKP(BC-DF) dataset, plotted as a function of  $\xi$  (Figure 13a), with predictions from two simple models of outer core heterogeneity of the type described above (Figure 13 bc). Both models are able to reproduce the characteristic L shape of the BC-DF trend as a function of angle  $\xi$ . The fit to individual data points depends on the details of the model, which we do not attempt to quantify any further here. Fits appear slightly

better if the cylinder is tilted about  $15^\circ$  with respect to the earth's rotation axis (Figure 13c). However, this may be an artefact due to uneven sampling, and to the fact that the real structure may be more complex than can be accounted for by such a simple model. Indeed, some models of the dynamics of the outercore indicate the presence of irregular vortices around the periphery of the tangent cylinder (e.g. J. Arnou, personal communication; Hulot et al., 2002), so that the detailed shape of the borders of the region of fast velocity may not be exactly cylindrical. Because the sam-



**Figure 11.** Location of the 6 south Sandwich Island earthquakes discussed in the text. Ray paths to the Alaska network are plotted, as well as the location of core entry points of PKP(DF) (diamonds), and PKP(BC) (triangles). Different colors are used to distinguish paths from different source locations. Only differential travel times were available for the event of 91/06/15.



**Figure 12.** Variations of PKP(BC-DF) relative travel time residuals as a function of distance for different south Sandwich Island events observed at stations of the Alaska network. a) 91/12/27, 91/06/15 and 91/12/28 events. ; b) data at stations COL and INK of the global seismic network; c) 04/07/25 and 93/03/20 events; d) 93/01/10 event.

pling of polar paths largely misses the central part of the tangent cylinder, it is not possible to determine if the whole volume of the latter would contain faster than average P velocity. The main point here is to illustrate that such a class of models is geometrically plausible. This is further emphasized in Figure 14, where we only show polar paths, separated according to whether the station or an event located in southern polar regions. One feature of the data is that both subsets thus obtained show an L shaped trend (as a function of  $\xi$ ), but the vertical portion of the L occurs in different  $\xi$  ranges (possibly due to uneven sampling). With slightly different cylindrical models, the trends in each of the subsets can be well reproduced. We note, in particular, that a simple model appears to also provide an explanation for the negative PKP(BC-DF) travel time anomalies around  $\xi \sim 45^\circ$  that correspond to a south Atlantic earthquake (93/03/29, lat =  $-52.96^\circ$ ; lon =  $27.37^\circ$ ; depth  $24.1\text{km}$ ) observed on the dense short period California networks, as measured by McSweeney et al. (1997).

Such a heterogeneous model of the outer core, related to structure in and/or around the tangent cylinder, is compatible with free oscillation splitting data (Romanowicz and

Bréger, 2000). An associated negative density anomaly of the order of  $-0.5\%$  inside the tangent cylinder has been suggested from normal mode data analysis (Widmer et al., 1992; Romanowicz and Bréger 2000), although it may be possible to fit normal mode data without any density anomaly in the outer core (Widmer et al., 1992). The physical plausibility of sustained lateral heterogeneity in the outer core is generally rejected on the basis of simple dynamical arguments in the vigorously convecting outer core (e.g. Stevenson, 1987). However, because the circulation within the tangent cylinder appears to be largely isolated from that outside of it (Hollerbach and Jones, 1995; Olson et al., 1999), one could imagine that light elements expelled from the inner core during crystallization might concentrate inside vortices in and around the tangent cylinder, giving rise to higher velocities. Whether or not the actual balance of forces allows a higher concentration of light elements in a region of the outercore, remains to be determined. At this point, both models proposed to explain first order features in the PKP travel time data: complex inner core anisotropy or outer core structure, present challenges for interpretation in terms of physical processes.

## 6. Conclusions

Our analysis of absolute and relative PKP travel time residuals on the global scale indicates that the hemispherical pattern previously documented in PKP(BC-DF) data is also present in PKP(AB-DF), and more significantly, in PKP(DF), a priori favoring an interpretation in terms of hemispherical anisotropy in the inner core, as has previously been proposed.

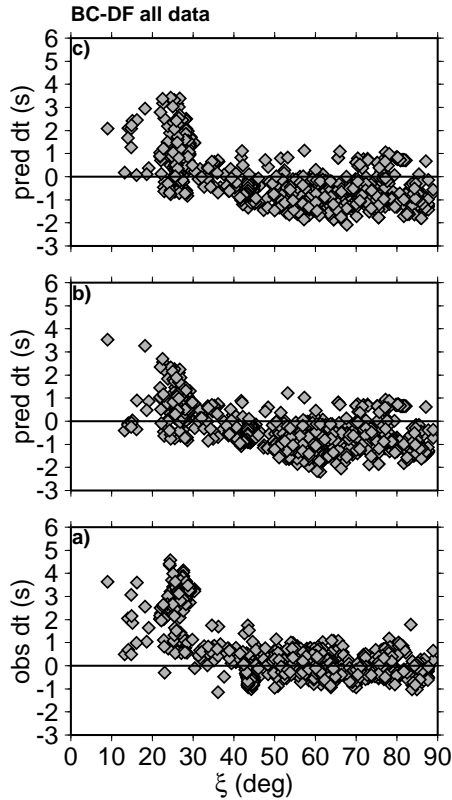


**Figure 13.** Observed (Bottom) and predicted (middle,top) PKP(BC-DF) travel time anomalies as a function of  $\xi$ , for two models involving cylindrical heterogeneity in the outer core. The P velocity is higher by 1% inside a cylinder of radius 1250 km surrounding the inner core, with, in b), axis parallel to the rotation axis, and in c) axis inclined towards lat =  $75^\circ N$ , lon =  $-110^\circ E$ . Both models explain over 50% of the variance in the data.

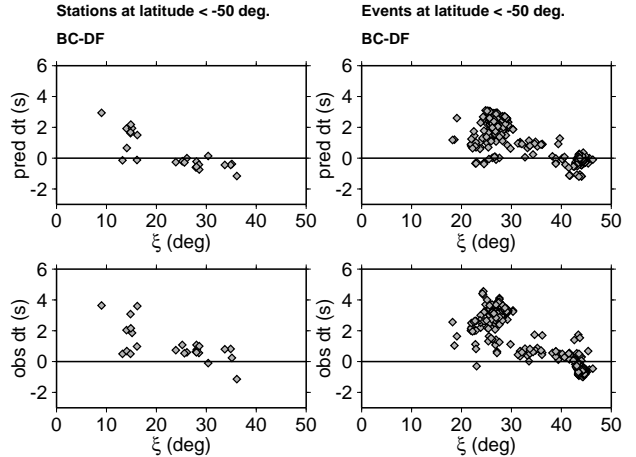


**Figure 14.** PKP(BC-DF) travel time residuals observed for polar paths. Left panels: paths corresponding to stations at latitudes  $< -50^\circ S$ ; right panels: paths corresponding to events at latitudes  $< -50^\circ S$ . Stations include SPA, SYO, PMSA, SNA and SBA. Events include earthquakes in the south Atlantic, southern Indian and south Pacific ocean. Bottom: observations; top: predictions for outercore models with 1% higher velocity inside a cylinder surrounding the inner core, of radius 1250 km, of axis pointing towards lat =  $75^\circ N$ , lon =  $-110^\circ E$  (top left) and lat =  $75^\circ N$ , lon =  $-170^\circ E$  (top right). The inclination of the cylinder may be an artifact due to the simplicity of the model. There are also no strong constraints on the structure in the central part of the cylinder.

It is not possible to explain this hemispherical pattern and its amplitude by a combination of realistic heterogeneity in the deep mantle and constant inner core anisotropy. The hemispherical anisotropy model is however difficult to explain physically, and also fails to explain the L-shaped pattern of PKP(BC-DF) residuals as a function of  $\xi$ , as well as the details of the distribution of residuals on south Sandwich to Alaska paths. The latter could indicate the presence of a thin, quasi-vertical fast velocity slab in the deep mantle. An alternative interpretation of the trends observed, in particular the L-shape in the trend of PKP(BC-DF) travel times as a function of  $\xi$ , could involve outer core structure in the vicinity of the inner core "tangent cylinder", an important feature in outer core dynamical models, which, in particular, exhibit separate circulation within and outside the tangent cylinder. Faster than average P velocity (by 0.8 to 1%) could arise inside the tangent cylinder and/or in vortices surrounding it (e.g. Hulot et al., 2002), and could be related to stronger concentration of light elements, as they are expelled from the inner core during crystallization. This interpretation also does not require the major departure from axial symmetry implied by the hemispherical inner core model. However, it is generally assumed that the outer core is well mixed, which does not allow any detectable heterogeneity in the outer core. Yet, such models do not account for effects of turbulence. As long as a valid physical explanation for strong non axial symmetry in the inner core, as implied by the hemispherical models, has not been found, such an alternative model may be of interest.

**Acknowledgments.** This paper was completed while BR was on sabbatical leave at the CNRS in Paris, France. We acknowledge partial support from NSF grant EAR#9902777. It is BSL contribution #02xx.

## References

- Bergman, M. I. Measurements of elastic anisotropy due to solidification texturing and the implications for the Earth's inner core, *Nature*, 389, 60-63, 1997.
- Bréger, L. and B. Romanowicz, Thermal and chemical 3D heterogeneity in D", *Science*, 282, 718-720, 1998.
- Bréger, L., B. Romanowicz, and H. Tkalčić, PKP(BC-DF) travel times: New constraints on short scale heterogeneity in the deep earth? *Geophys. Res. Lett.*, 26, 3169-3172, 1999.
- Bréger, L., H. Tkalčić and B. Romanowicz, The effect of D" on PKP(AB-DF) travel time residuals and possible implications for inner core structure, *EPSL*, 175, 133-143, 2000a.
- Bréger, L., B. Romanowicz and S. Rousset, New constraints on the structure of the inner core from P'P', *Geophys. Res. Lett.*, 27, 2781-2784, 2000b.
- Bréger, L., B. Romanowicz and C. Ng, The Pacific plume as seen by S, ScS, and SKS, *Geophys. Res. Lett.*, 25, 1859-1862.
- Buffett, B. A. and K. C. Creager, A comparison of geodetic and seismic estimates of inner-core rotation, *Geophys. Res. Lett.*, 26, 1509-1512, 1999.
- Creager, K.C., Anisotropy of the inner core from differential travel times of the phases PKP and PKIKP, *Nature*, 356, 309-314, 1992.
- Creager, K.C., Inner core rotation rate from small-scale heterogeneity and time-varying travel times, *Science*, 278, 1284-1288, 1997.
- Creager, K.C., Large-scale variations in inner core anisotropy, *J. Geophys. Res.*, 104, 23,127-23,139, 1999.
- Creager, K. C., Inner core anisotropy and rotation, in *Earth's deep interior: Mineral Physics and Seismic Tomography from the atomic to the global scale*, Geophysical Monograph 117, AGU, 2000.
- Durek, J. and B. Romanowicz, Inner core anisotropy inferred by direct inversion of normal mode spectra, *Geophys. J. Int.*, 139, 599-622, 1999.
- Dziewonski, A. M., B. Hager and R. J. O'Connell, Large scale heterogeneities in the lower mantle, *J. Geophys. Res.*, 82, 239-255, 1977.
- Engdahl, E. R., van der Hilst, R. D. and Buland, R. P., Global teleseismic earthquake relocation with improved travel times and procedures for depth determination, *Bull. Seismol. Soc. Am.*, 88, No 3, 722-743, 1998.
- Garcia, R. and A. Souriau, Inner core anisotropy and heterogeneity level, *Geophys. Res. Lett.*, 27, 3121-3124, 2000.
- Garnero, E. J. and D.V. Helmberger, Seismic detection of a thin laterally varying boundary layer at the base of the mantle beneath the Central-Pacific, *Geophys. Res. Lett.*, 23, 977-980, 1996.
- Grand, S.P., R. D. van der Hilst, and S. Widiyantoro, Global seismic tomography: a snapshot of convection in the earth, *GSA Today*, 7, 1-7, 1997.
- Hollerbach, R. and C. A. Jones, On the magnetically stabilizing role of the Earth's inner core, *Phys. Earth Planet. Inter.*, 87, 171-181, 1995.
- Hulot, G., C. Eymin, B. Langlais, M. Madea and N. Olsen, Small-scale structure of the geodynamo inferred from Oersted and Magsat satellite data, *Nature*, 416, 620-623, 2002.
- Jeanloz, R. and Wenk, H.R., Convection and anisotropy of the inner core, *Geophys. Res. Lett.*, 15, 72-75, 1988.
- Karason, H and R. D. van der Hilst, Tomographic imaging of the lowermost mantle with differential times of refracted and diffracted core phases (PKP, Pdiff), *J. Geophys. Res.*, 106, 6569-6587, 2001.
- Karato, S., Seismic anisotropy of the earth's inner core resulting from flow induced by Maxwell stresses, *Nature*, 402, 871-873, 1999.
- Karato, S., Inner core anisotropy due to magnetic field-induced preferred orientation of iron, *Science*, 262, 1708-1711, 1993.
- Li, X-D., D. Giardini, and J. H. Woodhouse, Large-scale three-dimensional even-degree structure of the Earth from splitting of long-period normal modes, *J. Geophys. Res.*, 96, 551-557, 1991.
- Liu, X. F. and A.M. Dziewonski, Global analysis of shear wave velocity anomalies in the lowermost mantle, in *The core-mantle boundary region*, Geodyn. ser. vol. 28, edited by M. Gurnis et al., pp 21-36, AGU, Washington, D.C., 1998.
- Masters, G. and F. Gilbert (1981) Structure of the inner core inferred from observations of its spheroidal shear modes, *Geophys. Res. Lett.*, 8, 569-571.
- Masters G., Johnson, S., Laske, G. and Bolton, B., 1996. A shear-velocity model of the mantle, *Philos. Trans. R. Soc. Lond. A*, 354, 1,385-1,411.
- McSweeney, T. J., K. C. Creager and R. T. Merrill, Depth extent of inner-core seismic anisotropy and implications for geomagnetism, *Phys. Earth Planet. Inter.*, 101, 131-156, 1997.
- Mégnin, C. and Romanowicz, B., 2000. The 3D shear velocity structure of the mantle from the inversion of body, surface, and higher mode waveforms, *Geophys. J. Int.*, 143, 709-728, 2000.
- Morelli, A., A.M. Dziewonski, and J. H. Woodhouse (1986) Anisotropy of the core inferred from PKIKP travel times, *Geophys. Res. Lett.*, 13, 1545-1548.
- Ni, S. and D. V. Helmberger, Low-velocity structure beneath Africa from forward modeling, *Earth Planet. Sci. Lett.*, 170, 497-507, 1999.
- Olson, P., U. Christensen and G. Glatzmeier, Numerical modeling of the geodynamo: mechanisms of field generation and equilibration, *J. Geophys. Res.*, 104, 10,383-10,404, 1999.
- Poupinet, G., R. Pillet and A. Souriau, Possible heterogeneity of the Earth's core deduced from PKIKP travel times, *Nature*, 305, 204-206, 1983.
- Ritsema, J., S. Ni, D. V. Helmberger, and H.P. Crotwell (1998) Evidence for strong shear velocity reductions and velocity gradients in the lower mantle beneath Africa, *Geophys. Res. Lett.*, 25, 4245-4248.
- Ritsema, J., H. van Heijst and J. Woodhouse, Complex shear wave velocity structure imaged beneath Africa and Iceland, *Science*, 286, 1925-1928, 1999.
- Ritzwoller, M., G. Masters, and F. Gilbert, Observations of anomalous splitting and their interpretation in terms of apherical structure, *J. Geophys. Res.*, 91, 10203-10228, 1988.

- Romanowicz, B. and L. Bréger, Anomalous splitting of free oscillations: a reevaluation of possible interpretations, *J. Geophys. Res.*, 105, 21,559-21,578, 2000.
- Romanowicz, B., X.-D. Li, and J. Durek, Anisotropy in the inner core; could it be due to low-order convection? *Science*, 274, 963-966, 1996.
- Sacks, I. S., Snoke, J. A. and Beach, L., 1979. Lateral heterogeneity at the base of the mantle revealed by observations of amplitudes of PKP phases, *Geophys. J. R. astr. Soc.*, **59**, 379-387.
- Shearer, P.M., K.M. Toy, and J.A. Orcutt, Axi-symmetric Earth models and inner core anisotropy, *Nature*, 333, 228-232, 1988.
- Shearer, P.M., PKP(BC) versus PKP(DF) differential travel times and aspherical structure in the Earth's inner core, *J. Geophys. Res.*, 96, 2233-2247, 1991.
- Song, X.-D., Anisotropy in central part of inner core, *J. Geophys. Res.*, 101, 16,089-16,097, 1996.
- Song, X.-D., Joint inversion for inner core rotation, inner core anisotropy and mantle heterogeneity, *J. Geophys. Res.*, 105, 7931-7943, 2000.
- Song, X.-D. and D.V. Helmberger, Seismic evidence for an inner core transition zone, *Science*, 282, 924-927, 1998.
- Souriau, A., P. Roudil and B. Moynot, Inner core differential rotation, facts and artefacts, *Geophys. Res. Lett.*, 24, 2103-2106, 1997.
- Stevenson, D. J., Limits on lateral density and velocity variations in the Earth's outer core, *Geophys. J. R. Astr. Soc.*, **88**, 311-319, 1987.
- Stixrude, L. and R. Cohen, High-pressure elasticity of iron and anisotropy of Earth's inner core, *Science*, 275, 1972-1975, 1995.
- Sylvander, M. and A. Souriau, P-velocity structure of the core-mantle boundary region inferred from PKP(AB)-PKP(BC) differential travel times", *Geophys. Res. Lett.*, 23, 853-856, 1996.
- Su, W. and A.M. Dziewonski, Inner core anisotropy in three dimensions, *J. Geophys. Res.*, 100, 9831-9852, 1995.
- Tanaka, S. and H. Hamaguchi, Degree one heterogeneity and hemispherical variation of anisotropy in the inner core from PKP(BC)-PKP(DF) times, *J. Geophys. Res.*, 102, 2925-2938, 1997.
- Tkalčić, H., B. Romanowicz and N. Houy, Constraints on D" structure using PKP(AB-DF), PKP(BC-DF) and PcP-P travel time data from broadband records, *Geophys. J. Int.*, **149**, 599-616, 2002.
- Vinnik, L., B. Romanowicz and L. Bréger, Anisotropy in the center of the Inner Core, *Geophys. Res. Lett.*, 21, 1671-1674, 1994.
- Tromp, J., Support for anisotropy of the Earth's inner core from splitting in free oscillation data, *Nature*, 366, 678-681, 1993.
- Tromp, J., Normal-mode splitting observations from the great 1994 Bolivia and Kuril Islands earthquakes: constraints on the structure of the mantle and inner core, *GSA Today*, 5, 137-151, 1995.
- Vinnik, L., Farra, V. and Romanowicz, B. Observational evidence for diffracted SV in the shadow of the Earth's core. *Geophys. Res. Lett.* **16**, 519-522, 1989.
- Widmer, R., G. Masters, and F. Gilbert, Observably split multiplets-data analysis and interpretation in terms of large-scale aspherical structure, *Geophys. J. Int.*, 111, 559-576, 1992.
- Woodhouse, J.H., D. Giardini, and X.-D. Li (1986) Evidence for inner core anisotropy from splitting in free oscillation data, *Geophys. Res. Lett.*, 13, 1549-1552.
- Wyssession, M. E., 1996. Large-scale structure at the core-mantle boundary from diffracted waves, *Nature*, **382**, 244-248.
- Yoshida, S., Sumita, I. & Kumazawa, M. Growth model of the inner core coupled with outer core dynamics and the resultant elastic anisotropy. *J. Geophys. Res.*, 101, 28085-28103, 1996.

---

B. Romanowicz, H. Tkalčić, L. Bréger, Berkeley Seismological Laboratory, Berkeley, CA, 94720, USA. (e-mail: barbara@seismo.berkeley.edu)

(Received \_\_\_\_\_)